

pointed out that a breakup of these "jets" into apparently still finer filaments, as is becoming apparent in Fig. 4(b), becomes even more pronounced at later times. On the other hand, depolarization from plasma density structures without magnetic field is possible,¹⁸ but how these structures could retain their form without any associated magnetic field is difficult to explain.

Although considerable density structure has been expected and observed in the underdense plasma and near critical density, we have presented results that show that the entire plasma displays very complicated density behavior during the rise of the CO₂-laser pulse. In addition we have found that plasma transport from the ablation layer is in our case dominated by instabilities in the overdense plasma that may well generate complex magnetic fields even in the underdense plasma. It therefore appears that stable adiabatic compression of laser targets is more difficult than foreseen, both to understand and to improve. Obviously more work needs to be done before an adequate knowledge of the problems in laser fusion is achieved.

¹T. P. Donaldson and I. J. Spalding, Phys. Rev. Lett. **36**, 467 (1976).

²D. T. Attwood, D. W. Sweeney, J. M. Auerbach, and P. H. Y. Lee, Phys. Rev. Lett. **40**, 184 (1978).

³J. F. Reintjes, T. N. Lee, R. C. Eckardt, and R. A. Andrews, J. Appl. Phys. **47**, 4457 (1976).

⁴R. Fedosejevs, I. V. Tomov, N. H. Burnet, G. D.

Enright, and M. C. Richardson, Phys. Rev. Lett. **39**, 932 (1977).

⁵H. Azechi, S. Oda, K. Tanaka, T. Norimatsu, T. Sasaki, T. Yamanaka, and C. Yamanaka, Phys. Rev. Lett. **39**, 1144 (1977).

⁶R. A. Haas, M. H. Boyle, K. R. Manes, and J. E. Swain, J. Appl. Phys. **47**, 1318 (1976).

⁷J. A. Stamper, E. A. Mclean, and B. H. Ripin, Phys. Rev. Lett. **26**, 1177 (1978).

⁸K. Estabrook, Phys. Fluids **19**, 1733 (1976); W. L. Kruer, E. J. Valeo, and K. G. Estabrook, University of California Radiation Laboratory Report No. UCRL-76612, 1975 (unpublished).

⁹R. P. Haas, H. D. Shay, W. L. Kruer, M. J. Boyle, D. W. Phillion, F. Rainer, V. C. Rupert, and H. N. Kornblum, Phys. Rev. Lett. **39**, 1533 (1977).

¹⁰G. Mitchel, B. Grek, F. Martin, H. Pépin, F. Rheault, and H. Baldis, to be published.

¹¹As SF₆ is a nonlinear absorber, it will tend to accentuate any nonuniformities of the laser beam.

¹²B. Grek, F. Martin, F. Rheault, and H. Pépin, to be published.

¹³F. J. Weinberg and N. B. Wood, J. Sci. Instrum. **36**, 227 (1959).

¹⁴C. M. Vest, Appl. Opt. **14**, 1601 (1975); M. M. Mueller, Los Alamos Scientific Laboratory Report No. LA-VR-77-2469, 1977 (unpublished).

¹⁵B. Grek, H. Pépin, T. W. Johnston, J. N. Leboeuf, and H. A. Baldis, Nucl. Fusion **17**, 1165 (1977).

¹⁶K. Mima, T. Tajima and J. N. Leboeuf, Phys. Rev. **41**, 1715 (1978).

¹⁷Y. V. A. Zakkarenkov, N. N. Zorev, O. N. Krokhin, Y. U. A. Mikhaslov, A. A. Rupajov, G. V. Sklizkov, and A. S. Shikanov, Zh. Eksp. Teor. Fiz. **70**, 547 (1976) [Sov. Phys. JETP **43**, 283 (1976)].

¹⁸R. Lemberg and J. Stamper, Phys. Fluids **21**, 814 (1978).

Retardation of Dislocation Generation and Motion in Thin-Layered Metal Laminates

S. L. Lehoczky

McDonnell Douglas Research Laboratories, McDonnell Douglas Corporation, St. Louis, Missouri 63166

(Received 2 August 1978)

The yield strengths of thin-layered Al-Cu and Al-Ag laminates greatly increase as the layer thicknesses are reduced. This strength enhancement is interpreted as evidence for the retardation of dislocation generation and motion as has been theoretically proposed.

Several years ago, Koehler¹ proposed that a laminate structure which is formed of thin layers of two metals, *A* and *B*, where one metal (*A*) has a high dislocation-line energy and the other metal (*B*) has a low dislocation-line energy, should exhibit a resistance to plastic deformation and brittle fracture well in excess of that for homogeneous alloys. If the dislocation-line energies are so mismatched, the termination of the motion of dislocations in metal *B* is energetically

favorable over a dislocation propagation across the layer interface into metal *A*. In the case of thick layers, the dislocations generated in either of the layers will pile up in *B* at the *B-A* interface and thereby provide the stress concentrations needed for premature yield. Hence, to suppress the generation of new dislocations in the layers, the thicknesses of *A* and *B* must be small.

In this Letter we report experimental results for the layer-thickness dependence of the yield

strength of Al-Cu and Al-Ag laminates. Below the critical layer thicknesses required for dislocation generation in the layers, the experimental results are in good agreement with Koehler's predictions. For layer thicknesses greater than those required for dislocation generation, we have extended the calculations to include dislocation-pileup groups. The calculated inverse layer-thickness dependence for the yield stress is in a good accord with the experimental data.

The Al-Cu and Al-Ag specimens were prepared by vapor deposition of the metals onto (100) NaCl single-crystal substrates maintained between 25 and 40°C. A micro tensile tester was used for all tensile measurements. The stress-loading rates were typically 1.8 MPa s⁻¹.

The experimental results for the layer-thickness dependence of the tensile yield stress for laminates having equal Al and Cu thicknesses are summarized in Fig. 1. The resolved tensile stress in the "soft" B layers at yield σ_a^B can be related to the measured tensile yield stress by the expression $\sigma_a^B = \sigma_a / (V_B + V_A Y_A / Y_B)$, where Y_A and Y_B are the Young's moduli, and V_A and V_B are the volume fractions of $A = \text{Cu, Ag}$ and $B = \text{Al}$, respectively. The data for the resolved tensile stress in the Al layers at yield, designated by solid triangles in Fig. 2, are for laminates that had 50-nm Cu layers and the range of Al-layer-

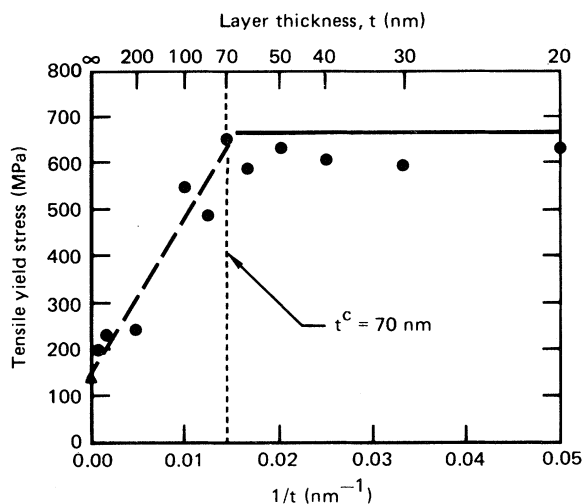


FIG. 1. Inverse layer-thickness dependence of the tensile yield stress for Al-Cu laminates. The Al- and Cu-layer thicknesses were equal in each laminate. The solid triangle is the value given by the rule of mixtures for thick films of the metals. The solid line is given by Eq. (4). The dashed line is given by Eq. (7) with $C_{\text{Cu}} = 0.75$ and $t_{\text{Cu}}^c = 70$ nm.

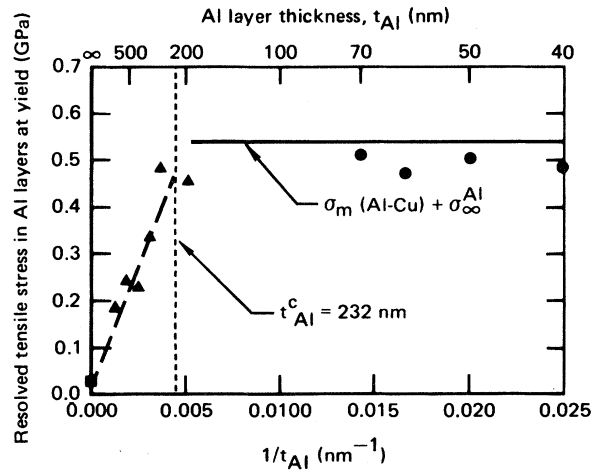


FIG. 2. Inverse Al-layer-thickness dependence of the resolved tensile stress in the Al layers at yield for Al-Cu laminates. For the data points denoted by solid triangles, the Cu-layer thicknesses were about 50 nm, and the Al-layer thicknesses were varied as indicated. The solid square denotes the value measured in "thick" Al films. The dashed line is given by Eq. (6) with $C_{\text{Al}} = 0.85$ and $t_{\text{Al}}^c = 232$ nm.

er thicknesses shown. The data in Fig. 3 are for Al-Ag laminates having nearly equal layer thicknesses. The values of the Young's moduli measured for thick films of each metal are given in

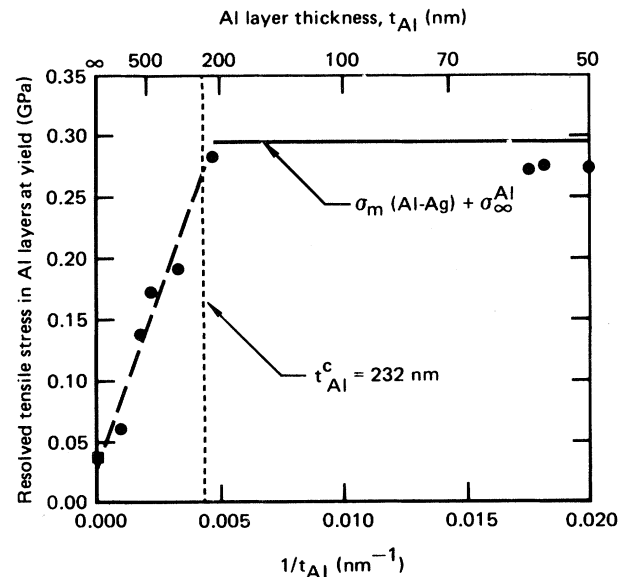


FIG. 3. Inverse Al-layer-thickness dependence of the resolved tensile stress in the Al layers at yield for Al-Ag laminates. The Al- and Ag-layer thicknesses were nearly equal in each laminate. The dashed line is given by Eq. (6) with $C_{\text{Al}} = 0.85$ and $t_{\text{Al}}^c = 232$ nm.

Table I. The stress values given in the figures correspond to the first significant deviations from linear stress-strain behavior and are averages for one to ten specimens of each layer thickness. For most cases, the scatter in the measured flow-stress values was less than $\pm 15\%$. The resolved tensile yield stress in the Al layers for each laminate system shows a large increase as the layer thickness decreases to some critical value, below which it is independent of layer thickness. A comparison of the results in Figs. 1 and 2 implies that the critical layer thicknesses were $t_{\text{Cu}}^c = 70$ and $t_{\text{Al}}^c = 232$ nm. The critical layer thickness for the Al-Ag system also is about 232 nm which probably again corresponds to the minimum thickness required for Frank-Read-type dislocation source operation in the Al layers.

Using isotropic-elasticity theory and boundary conditions similar to those considered by Head,² Koehler¹ gives the repulsive force per unit length between a screw dislocation in metal *B* and its nearest image in metal *A* as

$$F = R\mu_B b^2/4r, \quad (1)$$

where $R = (\mu_A - \mu_B)/(\mu_A + \mu_B)$, μ_A and μ_B are the respective moduli of rigidity of metals *A* and *B*, b is the Burgers displacement in *B*, and r is the distance between the dislocation and the nearest interface. He notes that the maximum repulsion should occur when $r = r_{\text{min}} \approx 2b$, and finds that the maximum interfacial repulsive shearing stress is given by

$$\sigma_m' = R\mu_B \sin\theta/8\pi = \sigma_m \sin\theta, \quad (2)$$

where, by definition, $\sigma_m = R\mu_B/8\pi$, and θ is the smallest angle between the interface and the glide plane of metal *B*. The resolved tensile stress in the *B* layers required for yield σ_a^B is therefore given by $\sigma_a^B \sin\theta \cos\theta = \sigma_m \sin\theta + \sigma_s^B$, where σ_s^B is the shearing stress required to overcome the frictional forces.

We approximate the minimum value of the resolved tensile stress required for grains having the most favorable glide-plane orientations for yield by the expression

$$\sigma_a^B \geq \sigma_m + \sigma_\infty^B, \quad (3)$$

where $\sigma_\infty^B = \sigma_a^B(t_B \rightarrow \infty)$ and t_B is the *B*-layer thickness. For the extreme limits $\sigma_s^B/\sigma_m \rightarrow 0$ and $\sigma_m/\sigma_s^B \rightarrow 0$, the expression reduces, respectively, to the proper minimum values, i.e., $\sigma_a^B = \sigma_m(\cos\theta \rightarrow 1)$ and $\sigma_a^B = \sigma_\infty^B = 2\sigma_s^B$ ($\theta = 45^\circ$), and somewhat underestimates the stresses required between the limits. Generally, the applied stress required should be greater than σ_a^B . In the elastic region of the stress-strain characteristics, for a given strain ϵ , the applied stress σ_a is distributed between the *A* and *B* layers according to $\sigma_a = V_B Y_B \epsilon + V_A Y_A \epsilon$, where Y_B and Y_A are the Young's moduli, and V_A and V_B are the volume fractions of *A* and *B*, respectively. The condition for yield in the laminate is given by $Y_B \epsilon \geq \sigma_a^B \approx \sigma_m + \sigma_\infty^B$. The tensile stress needed, therefore, is

$$\sigma_a \geq [V_B + V_A Y_A/Y_B](\sigma_m + \sigma_\infty^B). \quad (4)$$

The pertinent material parameters used in the computations and the calculated and measured values of the resolved tensile stress in the Al layers at yield for layer thicknesses less than the critical values are summarized in Table I. Following Koehler,¹ we have used the cubic elastic constants C_{44} at 25°C for the modulus of rigidity of each metal. The values of C_{44} are from Schmunk and Smith,³ Overton and Gaffney,⁴ and Bacon and Smith.⁵ The solid curves in Figs. 1–3 correspond to the yield stresses calculated from Eq. (3) or (4). For both the Al-Cu and Al-Ag systems, the agreement between the measured and calculated results is reasonably good. Had we considered only the highest measured yield-stress values instead of the averaged values for several specimens, the discrepancies between the meas-

TABLE I. Summary of the measured and calculated results. The values of Y and σ_∞ were determined from data for thick films of the metals.

Metal or metal pair	μ (GPa)	Y (GPa)	σ_∞ (GPa)	$\sigma_m(B-A)$ (GPa)	$\sigma_a^B(B-A)$ (calc.) (GPa)	$\sigma_a^B(B-A)$ (meas.) (GPa)	t^c (nm)
Al	28.3	69.0	0.023	~232
Cu	75.4	104	0.256	~70
Ag	46.1	70.7	0.053	> 240
Al-Cu	0.511	0.534	0.496	...
Al-Ag	0.269	0.292	0.275	...

ured and calculated results would have been insignificant. On the other hand, Eq. (3) tends to underestimate the minimum stresses required. In the case of Al-Cu, where $\sigma_{\infty}^{Al} = 2\sigma_s^{Al} = 0.023$ GPa, the angle for the optimum glide-plane orientation for yield is $\sim 15.5^\circ$ and $\sigma_a^{Al}(\text{Al-Cu}) = 0.574$ GPa, which is about 7% higher than the value deduced from Eq. (3). For Al-Ag, the optimum angle is $\sim 18.7^\circ$ and $\sigma_a^{Al}(\text{Al-Ag}) = 0.325$ GPa, or about 9% higher than the value given in Table I and Fig. 3. When noting the magnitude of the observed effects, the estimated (6–8)% errors in the experimental data, and the idealized treatment of the overall problem, differences arising from the above considerations are not significant.

In contrast to the Petch-type⁶ inverse-square-root variation commonly observed for the grain-size dependence of the yield stress in bulk metals, above the appropriate critical layer thicknesses, the stresses at yield for each laminate system show a linear dependence on the inverse layer thickness. We explain this usual thickness dependence as follows. The shearing stress re-

quired to operate a Frank-Read dislocation source is given by $\alpha\mu b/l$, where l is the dimension of the source and α is a proportionality constant of the order of unity. For layer thickness $\geq l$, the dislocations generated in either layer pile up in B to provide stress concentrations at the A - B interface of the order of $n_B(\sigma_{as}^B - \sigma_s^B)$, where n_B is the number of dislocations in the pileup group and σ_{as}^B is the shear component of the applied stress in a given glide plane of B . The condition for yield is given approximately by $n_B(\sigma_{as}^B - \sigma_s^B) = \sigma_m \sin\theta$. Consider first the case when the generation of new dislocations occurs primarily in B . The pileup group will provide a back stress on the operating sources given approximately⁷ by $n_B\mu b_B/2\pi L_B$, where L_B is the length of the pileup group. According to Mott's theory⁸ of dynamic generation of dislocations, once a source starts to operate, it will continue to operate until the stress around it is reduced by $\alpha\mu b_B/l_B$, i.e., until $\alpha\mu b_B/l_B \approx n_B\mu b_B/2\pi L_B$ or $n_B = 2\pi\alpha L_B/l_B$. Hence, for "thick" layers, by using the same approximations that were involved in the derivation of Eqs. (3) and (4), the condition for yield may be written as

$$\sigma_a = \left(\sigma_{\infty}^B + \frac{l_B \sigma_m}{2\pi\alpha L_B} \right) \left[V_B + V_A \frac{Y_A}{Y_B} \right], \quad t_B > t_B^c, \quad t_A < t_A^c, \quad (5)$$

where l_B is the dimension of dislocation sources in B and t_A is the thickness of A . If $L_B = \gamma t_B$ and $l_B = \beta t_B^c$, where γ and β are proportionality constants of the order of unity, the resolved tensile stress in B required for yield is

$$\sigma_a^B = \sigma_a \left[V_B + V_A \frac{Y_A}{Y_B} \right]^{-1} = \sigma_{\infty}^B + C_B \sigma_m \frac{t_B^c}{t_B}, \quad t_B > t_B^c, \quad t_A < t_A^c, \quad (6)$$

where $C_B = \beta/2\pi\alpha\gamma$. Equation (6) predicts the inverse layer-thickness dependence that is implied by the experimental data of Fig. 2. For $t_{Al}^c = 232$ nm, Eq. (6) can be fitted to the data of Fig. 2 with $C_{Al} = 0.85$.

When the generation of new dislocations occurs primarily in metal A , i.e., in the Cu layers in the case of Al-Cu, the meaning of the thickness dependence of the result is less certain. Assuming, however, that the back stress on the operating sources in A is also caused by the dislocation pileup at the A - B interface, the arguments used in deriving Eq. (6) give the condition for yield as

$$\sigma_a \approx \left(\sigma_{\infty}^A + C_A \frac{t_A^c}{t_A} \sigma_m \right) \left[V_A + V_B \frac{Y_B}{Y_A} \right], \quad t_A > t_A^c, \quad t_A^c \ll t_B^c, \quad (7)$$

where $\sigma_{\infty}^A(V_A + V_B Y_B/Y_A) = \sigma_a(t_A \rightarrow \infty)$, $C_A = \beta'/2\pi\alpha'\gamma'$, and α' , β' , and γ' are the appropriate proportionality constants for metal A . Equation (7) also implies a linear inverse-layer-thickness dependence. Fitting Eq. (7) to the data of Fig. 1 yields $C_{Cu} = 0.75$ if $t_{Cu}^c = 70$ nm.

The stress-strain characteristics of several 240-nm-thick Ag specimens were measured and were linear nearly to the fracture stress of 0.64 GPa; this implies that the critical minimum thickness for dislocation sources to operate in

Ag is greater than 240 nm. Thus, we conclude that the generation of new dislocations in the case of Al-Ag laminates occurred chiefly in the Al layers. Consequently, the ratio of the slopes of the inverse layer-thickness dependence of the resolved yield stresses in Figs. 2 and 3 should be precisely $\sigma_m(\text{Al-Cu})/\sigma_m(\text{Al-Ag})$ according to Eq. (6). The dashed curve shown in Fig. 3 was calculated with the values of the parameters C_{Al} and t_{Al}^c determined by the fit to the data for Al-Cu.

The agreement between the predicted and measured results is excellent. For Al-Ag where $Y_{Al}/Y_{Ag} \approx 1$, Eqs. (6) and (7) are formally equivalent; the fitting of the data would not be significantly altered if the Ag layers were the main sources of new dislocations.

In conclusion, it has been established that the observed strength enhancement in thin-layered Al-Cu and Al-Ag laminates is caused by the repulsive dislocation-image forces described by Koehler.¹ The laminate systems investigated consisted of polycrystalline layers with nearly random grain orientations, and consequently the individual layers present rather complex three-dimensional slip systems. The calculated results are therefore approximate for they do not include the rigorous angular dependences of the forces acting in the possible glide planes.

The author is indebted to R. L. Wyatt for his invaluable technical assistance in the experimental

work and is also greatly thankful to C. R. Whitsett and D. P. Ames of the McDonnell Douglas Research Laboratories and W. T. Highberger of the Naval Air Systems Command for their many illuminating discussions of the problem. This research was supported by the U. S. Department of the Navy, Naval Air Systems Command.

¹J. S. Koehler, Phys. Rev. B 2, 547 (1970).

²A. K. Head, Proc. Phys. Soc., London, Sect. B 66, 793 (1953), and Philos. Mag. 44, 92 (1953).

³R. E. Schmunk and C. S. Smith, J. Phys. Chem. Solids 9, 100 (1959).

⁴W. C. Overton, Jr., and J. Gaffney, Phys. Rev. 98, 969 (1955).

⁵R. Bacon and C. S. Smith, Acta Metall. 4, 337 (1956).

⁶W. J. Petch, J. Iron Steel Inst. 173, 25 (1953).

⁷J. Friedel, *Dislocations* (Addison-Wesley, Reading, Mass., 1964), p. 261.

⁸N. F. Mott, Philos. Mag. 43, 1151 (1952).

Dynamic Scaling near the Lambda Point in Liquid Helium

Richard A. Ferrell

Institute for Physical Science and Technology and Department of Physics and Astronomy, University of Maryland, College Park, Maryland 20742

and

Volker Dohm

Department of Physics and Astronomy, University of Maryland, College Park, Maryland 20742,^(a) and Institut für Festkörperforschung, Kernforschungsanlage Jülich, 517 Jülich, Germany^(b)

and

Jayanta K. Bhattacharjee

Department of Physics and Astronomy, University of Maryland, College Park, Maryland 20742

(Received 5 July 1978)

Two-loop calculations indicate that the order parameter in liquid helium at the λ point may relax by an order of magnitude more slowly than the entropy. Consequently the critical region for entropy relaxation is expanded by an order of magnitude, both above and below the λ point, which may help to reconcile light-scattering data, second-sound damping, and dynamic scaling theory. Characteristic double-humped spectra are calculated, providing a crucial test of the present theory.

From general considerations a dynamic scaling theory^{1,2} has been advanced in which it has been argued that the breadth of the spectrum of entropy fluctuations at the λ point in liquid helium scales with wave number k according to

$$\omega_c(k) = ak^{3/2}. \quad (1)$$

Equation (1) has subsequently been confirmed by both the mode-coupling³ and dynamic renormalization-group theories.⁴ The value of the con-

stant a which is obtained from these theories compares satisfactorily with the value determined experimentally from light scattering by Winterling, Holmes, and Greytak,⁵ Vinen *et al.*,⁶ and Tarvin, Vidal, and Greytak.⁷ The temperature dependence predicted by dynamic scaling has, however, been found to be in gross contradiction with the experimental observations. In this note we offer an explanation of this discrepancy and show how dynamic scaling theory can